# Tris(2,2'-bipyridine)ruthenium(II)-Sensitized Photooxidation of Phenols. Environmental Effects on Electron Transfer Yields and Kinetics[1]

**K. Miedlar[2] and P. K. Das***

*Contribution from the Radiation Laboratory, University of Notre Dame, Notre Dame, Indiana 46556.* *Received March 29, 1982*

**Abstract:** Laser flash photolysis (337.1 nm) combined with kinetic absorption–emission spectrophotometry has been used to study the photoreduction of tris(2,2'-bipyridine)ruthenium(II) by a series of phenols with special emphasis on the effects of solvent, temperature, and ionic strength on electron transfer kinetics and yields. The excited-state quenching rate constants ($k_q$) are in the range $1 \times 10^6$–$5 \times 10^9$ $M^{-1}$ $s^{-1}$ for substituted phenolate ions (at pH 12.7) and correlate well with Hammett $\sigma^+$ values as well as with oxidation potentials. The plot of $RT \ln k_q'$ against $E_{ArO\cdot/ArO^-}$ has a slope of −0.5, $k_q'$ being the quenching rate constant corrected for the initial diffusional process. Arrhenius plots for $k_q$ in the cases of $p$-$CH_3O$–$C_6H_4O^-$, $C_6H_5O^-$, and $p$-$COO^-$–$C_6H_4O^-$ as quenchers in aqueous solutions are linear in the temperature range 0–80 °C and give 4.2, 8.1, and 12.8 kcal/mol, respectively, as apparent activation energies. With $p$-methoxyphenolate ion and $p$-methoxy-$N,N$-dimethylaniline as quenchers, $k_q$ increases on changing solvent from water to 95% ethanol or 95% acetone (both aqueous); this increase, however, is not monotonous as evident from $k_q$ going through a minimum at intermediate solvent compositions. The electron transfer yields ($\eta$) are in the range 0.3–1.0 for various phenolate ions in aqueous solutions (at pH 12.7). As observed with $p$-methoxyphenolate ion and $p$-methoxy-$N,N$-dimethylaniline, $\eta$ exhibits an increasing trend at elevated temperatures, in aqueous solvent systems richer in the nonaqueous component (acetone or ethanol), and at lower ionic strengths. This study also reports on the excited-state absorption spectrum (triplet–triplet) of tris(2,2'-bipyridine)ruthenium(II) in aqueous solution in the spectral region 230–800 nm showing small but nonnegligible spectral absorption at long wavelengths (500–800 nm) in addition to a prominent three-band feature at short wavelengths (240–400 nm).

## Introduction

Because of their potential application in solar energy storage and conversion, electron transfer reactions from and to the triplet metal-to-ligand charge transfer excited state of tris(2,2'-bipyridine)ruthenium(II) complex, $*Ru(bpy)_3^{2+}$, have been studied[3] quite extensively in recent years. A variety of electron donors and acceptors, both organic and inorganic, have been used in these reactions. Except in the cases[3a,m,4,5] where energy transfer occurs, the redox nature[3,6-8] of the quenching behavior of $*Ru(bpy)_3^{2+}$ has been established on the basis of steady-state photochemistry as well as flash-photolytic transient measurements.

Electron and hydrogen abstraction reactions involving phenols and related compounds (e.g., quinones) are of interest by virture of their important roles as antioxidants[9] and polymer photostabilizers,[10] and in biological redox systems. Previous reports[11] from this laboratory have dealt with kinetic and mechanistic aspects of photooxidation of phenols and phenolate ions sensitized by photochemically generated carbonyl triplets and *tert*-butoxy radicals. The present work is a result of our continued interest in the area of photoinduced electron transfer reactions involving phenols. Based primarily on 337.1-nm laser flash photolysis and nanosecond kinetic spectrophotometry, it has made use of $*Ru(bpy)_3^{2+}$ as a model excited-state acceptor for electrons originating from a series of monohydric, substituted phenolate ions with slowly varying redox potentials. Emphasis has been given on environmental effects in relationship with the rates and the yields of electron transfer and on the back-reaction among the photoredox products, namely, $Ru(bpy)_3^+$ and phenoxy radical (formed in relatively large yields). The kinetic and yield data are discussed in the light of current theories of electron transfer reactions. It is noted that, relative to the previous analogous studies[3c,f,8,12] using nitroaromatics and pyridinium ions for oxidative quenching and aromatic amines for reductive quenching, one important difference offered by the phenolate ions lies in the charge-to-charge electrostatic interactions among the reacting partners forming the electron-transfer-derived ion–radical pair in the solvent cage and among the products separating from it with or without back-transfer.

## Experimental Section

The majority of the phenols used in this study were obtained from Aldrich or Eastman and were purified by recrystallization, vacuum sublimation, or vacuum distillation. The solids were stored in a vacuum desiccator after purification. The following phenols were used as received: $p$-cresol (Aldrich), $m$-cresol (Aldrich), $m$-methoxyphenol (Fluka), $m$-fluorophenol (Aldrich), and $m$-cyanophenol (Aldrich). $p$-Meth-

(1) The work described herein is supported by the Office of Basic Energy Sciences of the Department of Energy. This is Document No. NDRL-2339 from the Notre Dame Radiation Laboratory.

(2) Undergraduate Research Fellow, Summer 1981, from Saint Mary's College, Notre Dame, IN 46556.

(3) A representative cross section of recent references is as follows: (a) Creutz, C.; Chou, M.; Netzel, T. L.; Okumura, M.; Sutin, M. *J. Am. Chem. Soc.* **1980**, *102*, 1309–19. (b) Young, R. C.; Keene, F. R.; Meyer, T. J. *Ibid.* **1977**, *99*, 2468–73. (c) Bock, C. R.; Connor, J. A.; Gutierrez, A. R.; Meyer, T. J.; Whitten, D. G.; Sullivan, B. P.; Nagle, J. K. *Ibid.* **1979**, *101*, 4815–24. (d) Lin, C.-T.; Sutin, N. *J. Phys. Chem.* **1976**, *80*, 97–104. (e) Gafney, H. D.; Adamson, A. W. *J. Am. Chem. Soc.* **1972**, *94*, 8238–9. (f) Amouyal, E.; Zidler, B.; Keller, P.; Moradpour, A. *Chem. Phys. Lett.* **1980**, *74*, 314–7. (g) Darwent, J. R.; Kalyansundaram, K. *J. Chem. Soc., Faraday Trans.* **1981**, *77*, 373–82. (h) Sutin, N. *J. Photochem.* **1979**, *10*, 19–40. (i) Maestri, M.; Grätzel, M. *Ber. Bunsenges. Phys. Chem.* **1977**, *81*, 504–7. (j) Brown, G. M.; Brunschwig, B. S.; Creutz, C.; Endicott, J. F.; Sutin, N. *J. Am. Chem. Soc.* **1979**, *101*, 1298–300. (k) Meyer, T. J.; Nagle, J. K.; Young, R. C. *Inorg. Chem.* **1977**, *16*, 3366–9. (l) Rodgers, M. A. J.; Becker, J. C. *J. Phys. Chem.* **1980**, *84*, 2762–8. (m) Balzani, V.; Moggi, L.; Manfrin, M. F.; Bolletta, F.; Laurence, G. S. *Coord. Chem. Rev.* **1975**, *15*, 321–433. (n) Whitten, D. G. *Acc. Chem. Res* **1980**, *13*, 83–90.

(4) (a) Bolleta, F.; Maestri, M.; Balzani, V. *J. Phys. Chem.* **1976**, *80*, 2499–503. (b) Juris, A.; Gandolfi, M. T.; Manfrin, M. F.; Balzani, V. *J. Am. Chem. Soc.* **1976**, *98*, 1047–8.

(5) Natarajan, P.; Endicott, J. F. *J. Phys. Chem.* **1973**, *77*, 971–2, 1823–1830; *J. Am. Chem. Soc.* **1973**, *95*, 2470–7; **1972**, *94*, 3635–6, 5909–10.

(6) (a) Navon, G.; Sutin, N. *Inorg. Chem.* **1974**, *13*, 2159–64. (b) Creutz, C.; Sutin, N. *J. Am. Soc.* **1976**, *98* 6384–5.

(7) Anderson, C. P.; Salmon, D. J.; Meyer, T. J.; Young, R. C. *J. Am. Chem. Soc.* **1977**, *99*, 1980–2.

(8) Bock, C. R.; Meyer, T. J.; Whitten, D. G. *J. Am. Chem. Soc.* **1975**, *97*, 2909–11.

(9) Scott, G. "Atmospheric oxidation and Antioxidants"; Elsevier: New York, 1965.

(10) Hodgeman, D. K. C. *Polym. Degradation Stab.* **1979**, *1*, 155 and references therein. Carlsson, D. J.; Suprunchuk, T.; Wiles, D. M. *J. Polym. Sci.* **1972**, *16*, 615–26.

(11) (a) Das, P. K.; Encinas, M. V.; Scaiano, J. C. *J. Am. Chem. Soc.* **1981**, *103*, 4154–62. (b) Das, P. K.; Encinas, M. V.; Steenken, S.; Scaiano, J. C. *Ibid.* **1981**, *103*, 4162–6. (c) Das, P. K.; Bhattacharyya, S. N. *J. Phys. Chem.* **1981**, *85*, 1391–5.

(12) Bock, C. R.; Connor, J. A.; Gutierrez, A. R.; Meyer, T. J.; Whitten, D. G.; Sullivan, B. P.; Nagle, J. K. *Chem. Phys. Lett.* **1979**, *61*, 522–5.

0002-7863/82/1504-7462$01.25/0 

oxy-*N*,*N*-dimethylaniline was prepared from *p*-methoxyaniline (Aldrich) by methylation with trimethyl phosphate according to the procedure given in the literature[13] and the crude product was purified by sublimation (twice) under vacuum. The solvents were obtained as follows: water (doubly purified by a Millipore Milli-Q system), ethanol (absolute, Aaper Alcohol and Chemical Co., distilled over magnesium turnings), and acetone (Fisher, spectrophotometric).

Tris(2,2′-bipyridine)ruthenium(II) dichloride hexahydrate, purchased from G. Frederick Smith Chemical Co., was used without further purification. The luminescence spectra and lifetimes and the absorption spectra in water were practically identical with those described in the literature and did not show any change on increasing pH from 7 to 13. Experiments repeated with Ru(bpy)$_3^{2+}$, recrystallized from water, showed no difference in the results regarding spectral and photophysical characteristics and quenching rate constants (observed with phenolate and *p*-methoxyphenolate ions).

The experiments concerning laser flash photolysis and kinetic analysis of resultant transient absorption and emission were carried out in a computer-controlled setup described elsewhere[11,14] using, for excitation, nitrogen laser pulses (337.1 nm, 8 ns, 2–3 mJ) from a Molectron UV-400 system. The kinetic spectrophotometer consisting of a pulsed xenon lamp (Osram 450 W), a high-intensity B & L monochromator (UV–visible), and an RCA 4840 (or R666S) photomultiplier tube permits routine measurements of transient phenomena (with lifetimes in the range 20 ns–50 μs) based on absorption or luminescence in the spectral region 300–700 nm. Under certain circumstances, the monitoring spectral region can be extended to 230–800 nm by using higher transient voltage from the pulser and larger band-pass in the monochromator. The direction of the exciting laser pulse is at ~20° to that of the monitoring beam.

The steady-state luminescence measurements were carried out in a spectrofluorimeter (photon counting) from SLM Corp.; the main features of this setup are given elsewhere.[15] For ground-state absorption spectra, a Cary 219 spectrophotometer was used at a band-pass of 1 nm.

All laser flash photolysis experiments were performed in Suprasil quartz cells of 3-mm path length using solutions that were deaerated by bubbling argon. The concentrations of Ru(bpy)$_3^{2+}$ and the quenchers were in the ranges 0.2–0.1 and 0.1–40 mM, respectively; the actual concentrations used for a particular experiment and for a particular system were dictated by the experimental parameter to be determined, viz., quenching rate constant ($k_q$) or electron transfer yield ($\eta$), as well as by the relative absorbances of the quenchers at 337.1 nm and the magnitudes of corresponding $k_q$'s. For instance, to obtain $\eta$, we kept the concentration of Ru(bpy)$_3^{2+}$ generally high (0.1–0.2 mM) to minimize screening of the laser light by the quenchers whereas the solutions used to measure $k_q$ were usually ~10 times dilute in Ru(bpy)$_3^{2+}$ (except in the cases where the quencher absorption at 337.1 nm was relatively high while $k_q$ was relatively small). For variable-temperature studies, a double-walled Dewar-type jacket with optically flat quartz windows was mounted around the photolysis cell and a regulated flow of hot or cold nitrogen was maintained through it around the cell. The nitrogen gas was either preheated by passing through a quartz column packed with quartz wool and heated in a tubular electric furnace or precooled by passing through a copper spiral tube immersed in liquid nitrogen. By controlling the flow of nitrogen, we could maintain the temperature within ±1 °C.

## Results

**Absorption Spectrum of Tris(2,2′-bipyridine)ruthenium(II) Triplet Excited State.** For electron transfer reactions from phenolate ions, the experiments had to be done in solutions at a relatively high pH (12–13). Thus, it became pertinent in the present study to establish that the spectral and photophysical features of *Ru(bpy)$_3^{2+}$ remain essentially unchanged in the basic media. As mentioned in the Experimental Section, the absorption–emission spectra, phosphorescence quantum yield, and lifetimes do not show any difference at high pH relative to an aqueous solution at pH 7. In addition, we have determined the excited-state (triplet–triplet) absorption spectrum of Ru(bpy)$_3^{2+}$ in the spectral region 240–800 nm in order to show that the spectrum remains unchanged in both location and extinction coefficient over the pH range 7–13 as well as to reveal some features not noted in the previously published[3a,16,17] spectra.

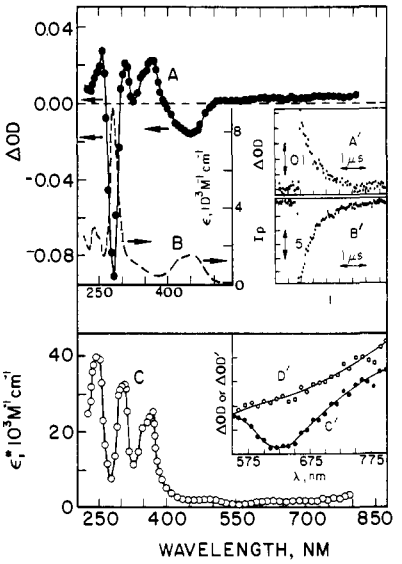


**Figure 1.** (A) Difference absorption spectrum, obtained at ~50 ns following laser flash, in terms of observed absorbance changes, of Ru(bpy)$_3^{2+}$ excited state in aqueous solution containing 0.05 M NaOH. (B) Ground-state absorption spectrum of Ru(bpy)$_3^{2+}$ in aqueous solution. (C) Excited-state absorption spectrum of Ru(bpy)$_3^{2+}$ in aqueous solution after correction for ground-state depletion, assuming excited-state extinction coefficient of 25 000 M$^{-1}$ cm$^{-1}$ at 368 nm. Insets: (A′) Experimental trace for triplet absorption decay, not corrected for phosphorescence, at 740 nm. (B′) Experimental trace for phosphorescence decay alone at 740 nm with monitoring lamp "off". (C′) Difference absorption spectrum not corrected for contribution of phosphorescence, at 500–800 nm. (D′) Difference absorption spectrum at 500–800 nm after correction for phosphorescence.

Figure 1 illustrates various aspects of the triplet–triplet absorption spectrum of Ru(bpy)$_3^{2+}$ observed in aqueous solution at pH 12.7. Figure 1A (difference spectrum) shows the absorbance

(13) Thomas, D. G.; Billman, J. H.; Davis, C. E. *J. Am. Chem. Soc.* **1946**, *68*, 895–6. Billman, J. H.; Radike, A.; Mundy, B. W. *Ibid.* **1942**, *64*, 2977–8.
(14) Das, P. K.; Bobrowski, K. *J. Chem. Soc., Faraday Trans. 2* **1981**, *77*, 1009–27.
(15) Chattopadhyay, S. K.; Das, P. K.; Hug, G. L. *J. Am. Chem. Soc.* **1982**, *104*, 4507–14.
(16) (a) Bensasson, R.; Salet, C.; Balzani, V. *J. Am. Chem. Soc.* **1976**, *98*, 3722–4; (b) *Hebd. C. R. Seances Acad. Sci., Ser. B* **1979**, *289*, 41–3.
(17) Lachish, V.; Infelta, P. P.; Grätzel, M. *Chem. Phys. Lett.* **1979**, *62*, 317–9.
(18) Dallinger, R. F.; Woodruff, W. H. *J. Am. Chem. Soc.* **1979**, *101*, 4391–3. Bradley, P. G.; Kress, N.; Hornberger, B. A.; Dallinger, R. F.; Woodruff, W. H. *Ibid.* **1981**, *103*, 7441–6.
(19) Mahon, C.; Reynolds, W. L. *Inorg. Chem.* **1967**, *6*, 1927.
(20) Weston, R. E.; Schwarz, H. A. "Chemical Kinetics"; Prentice-Hall: Englewood Cliffs, NJ, 1972.
(21) (a) Rehm, D.; Weller, A. *Ber. Bunsenges. Phys. Chem.* **1969**, *73*, 834–9; (b) *Isr. J. Chem.* **1970**, *8*, 259–71.
(22) Strictly speaking, expression 4 for $k_q$ is applicable only when $k_q$ is measured from Stern–Volmer plots based on steady-state luminescence quenching. For measurements based on observation of transient kinetics following pulsed excitation, as used in the present study, expressions 4 and 5 can be derived if steady-state assumptions are applied for the intermediates A and B (see Scheme I). The fact that the decay of *Ru(bpy)$_3^{2+}$ was found to be a single exponential (first-order) process even at the highest [Q]'s suggests the dominance of one exponential term in the overall transient process (which, in principle, contains three exponential terms based on Scheme I). This, coupled with the facts that $k_{obsd}$ is found to be the same whether it is determined from *Ru(bpy)$_3^{2+}$ decay or from photoproduct(s) formation and that the plots of $k_{obsd}$ vs. [Q] are linear, leads us to conclude that expressions 4 and 5 (for $k_q$ and $\eta$, respectively) are applicable within our experimental errors. Further support of this conclusion comes from the comparison of $k_q$'s measured in specific cases by both steady-state quenching and transient kinetics; the discrepancy between $k_q$'s obtained by the two methods was random, and within experimental errors.
(23) $E_{T_1}$ of phenol is 81.7 kcal/mol.[24] Parallel to the red shifting of $S_1$ on going from phenol to phenolate ion and on substitution in the ring, one would expect $E_{T_1}$ to be lower in the substituted phenolate ions. However, in any case, the magnitude of the lowering of $E_{T_1}$ is expected to be much less than 30 kcal/mol.
(24) McClure, D. S. *J. Am. Chem. Soc.* **1949**, *17*, 905–13.
(25) $k_{12}$ is calculated from the Smoluchowski equation modified by Debye for reactions between ions in an electrolyte solution (Debye, P. *Trans. Electrochem. Soc.* **1942**, *82*, 265–72). In water at 23 °C ($\mu$ = 0.05), the value obtained for $k_{12}$ is 8.9 × 10$^9$ M$^{-1}$ s$^{-1}$ for Ru(bpy)$_3^{2+}$ and ArO$^-$, using radii 7.1 and 3.8 Å for the two reactants, respectively (in keeping with parameters used in previous studies[3c,12]).

change (Δ(OD)), observed at ~50 ns following laser flash, as a function of wavelength. This was obtained by normalizing and combining three portions of the spectrum determined in separate experiments using different $Ru(bpy)_3^{2+}$ concentrations for the three spectral regions, namely, $2 \times 10^{-5}$ M for 240–400 nm, $1 \times 10^{-4}$ M 350–550 nm, and $2 \times 10^{-4}$ M for 500–800 nm. Such adjustment of concentrations was necessary to avoid complete absorption of the monitoring light by ground-state $Ru(bpy)_3^{2+}$. Note that the observed Δ(OD)'s in the long-wavelength region (550–800 nm) are distorted because of the contribution of phosphorescence ($I_P$). In fact, when the monitoring lamp intensity ($I_0$) is relatively low, negative values are obtained for apparent Δ(OD)'s at 590–640 nm because of the dominance of phosphorescence ($I_P$) at these wavelengths over the intensity ($I_S$) of light absorbed by $*Ru(bpy)_3$. In order to make $I_S$ large enough to dominate over $I_P$ as well as to obtain sufficient $I_0$ at very long wavelengths (700–800 nm), we enhanced the monitoring lamp intensity by a factor of 3–4 by increasing the transient voltage furnished by the lamp pulser. Also, for 700–800 nm, the monochromator slits were opened for a wider band-pass (10–20 nm).

The apparent Δ(OD)'s at 550–800 nm were corrected for the contribution of phosphorescence by measuring the signal corresponding to it at each wavelength with the monitoring lamp blocked by a shutter and subtracting it algebraically from the combined signal due to phosphorescence and triplet–triplet absorption. The insets A′ and B′ of Figure 1 show two typical traces at 730 nm with the monitoring lamp "on" and "off", respectively. The spectra C′ and D′ in the bottom inset of Figure 1 illustrate how the apparent Δ(OD)'s (uncorrected for phosphorescence, Figure 1C′) change after the correction is applied (Figure 1D′).

In Figure 1A, Δ(OD) at a particular wavelength is proportional to $\epsilon^* - \epsilon^g$ where $\epsilon^*$ and $\epsilon^g$ are the extinction coefficients of $Ru(bpy)_3^{2+}$ in the excited and ground states, respectively, at this wavelength. The ground-state absorption spectrum is shown in Figure 1B. Most of the reported values[3a,16a,17] for the extinction coefficient of $*Ru(bpy)_3^{2+}$ absorption at 360–370 nm are in the range 25 000–27 000 $M^{-1}$ $cm^{-1}$. Using a value of 25 000 $M^{-1}$ $cm^{-1}$ for $\epsilon^*$ at 368 nm, we obtained the complete absorption spectrum at 230–800 nm, shown in Figure 1C. It is noted that, because of strong overlap with the ground-state absorption band system at 400–500 nm, the excited-state absorption spectrum in this spectral region is sensitive to the value chosen for $\epsilon^*$ at 368 nm. On the basis of Δ(OD) data in Figure 1A, we find that the excited-state absorption intensity would be practically nil at 450–500 nm, if $\epsilon^*$ at 368 nm is taken to be 27 000 $M^{-1}$ $cm^{-1}$. On the other hand, if a value[26b] of 14 000 $M^{-1}$ $cm^{-1}$ is chosen for $\epsilon^*$ at 368 nm, $\epsilon^*$ at 450 nm will be 9000 $M^{-1}$ $cm^{-1}$.

The three-band pattern for $*Ru(bpy)_3^{2+}$ absorption in the short-wavelength region (230–400 nm) with maxima at 255, 310, and 368 nm, respectively, agrees very well with the spectrum reported[17] by Lachish, Infelta, and Grätzel, in terms of both location and relative intensity. The assignment of these band systems should be of interest particularly in view of the current resonance Raman spectral evidence[18] demonstrating that, in the triplet charge transfer excited state of $Ru(bpy)_3^{2+}$, the electron transferred from the metal center is localized on one of the 2,2′-bipyridine ligands. Thus, while the 368-nm band is associated with the ligand with anionic character on the basis of its similarity (in location) with the spectrum of 2,2′-bipyridine radical anion,[19] the higher-energy bands, particularly the one at 310 nm, may very well be related with the bpy ligands having no anionic character.

The portion of the $*Ru(bpy)_3^{2+}$ spectrum between 500 and 800 nm, reported here for the first time, shows clearly that the spectral absorption in this wavelength range, though small, is nonnegligible. As a matter of fact, the spectral absorption intensity (Figure 1A,C) shows an increasing trend at very long wavelengths (750–800 nm).

(26) (a) Marcus, R. A. *J. Chem. Phys.* **1965**, *43*, 679–701. (b) Marcus, R. A.; Sutin, N. *Inorg. Chem.* **1975**, *14*, 213–9. (c) Hush, N. S. *Trans. Faraday Soc.* **1961**, *57*, 557–80.

(27) Scandola, F.; Balzani, V. *Z. Am. Chem. Soc.* **1979**, *101*, 6140–2. Balzani, V.; Scandola, F.; Orlandi, G.; Subbatani, N.; Indelli, M. T. *Ibid.* **1981**, *103*, 3370–8.

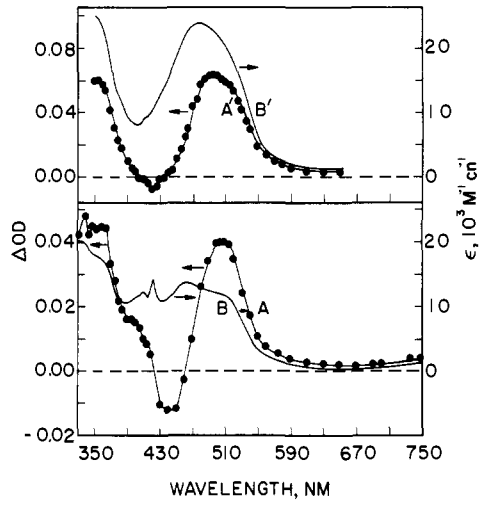


**Figure 2.** (A) Difference absorption spectrum for combined photoproducts for $Ru(bpy)_3^{2+}$ + *p*-methoxyphenolate ion system in aqueous solution at pH 12.7 (observed after completion of $*Ru(bpy)_3^{2+}$ decay). (B) Absorption spectra of the photoproducts in the same system as in A, after correction for ground-state depletion and assuming an extinction coefficient of 12 000 $M^{-1}$ $cm^{-1}$ due to $Ru(bpy)_3^{+}$ at 510 nm. (A′) Difference absorption spectra of photoproducts in the case of $Ru(bpy)_3^{2+}$ + *p*-methoxy-*N*,*N*-dimethylaniline system in aqueous solution at pH 7. (B′) Absorption spectra of photoproducts in the same system as in A′ after correction for ground-state absorption and assuming $\epsilon$ = 12 000 $M^{-1}$ $cm^{-1}$ for $Ru(bpy)_3^{+}$ and $\epsilon$ = 8000 $M^{-1}$ $cm^{-1}$ for *p*-methoxy-*N*,*N*-dimethylaniline radical cation at 510 nm.

Even with relatively weak monitoring light intensity and low sensitivity of detector system, we could obtain reasonably good experimental traces for the decay of triplet–triplet absorption of $Ru(bpy)_3^{2+}$ at 750–800 nm. Our result suggests the existence of transition(s) at very low energies and calls for proper consideration in the complete assignment of excited states in this system. It should be noted that 2,2′-bipyridine radical anion also has weak spectral absorptions at very long wavelengths with $\epsilon$'s 900 and 600 $M^{-1}$ $cm^{-1}$ at 840 and 750 nm, respectively.[19]

**Rate Constants for Reductive Quenching of $*Ru(bpy)_3^{2+}$ by Phenolate Ions.** The presence of phenolate ions (at pH 12–13) and some of the phenols (at pH 7) in a $Ru(bpy)_3^{2+}$ solution results in the decrease of steady-state phosphorescence intensity as well as in the shortening of excited-state lifetime. That the quenching is reductive is shown by the formation of photoproducts that are identifiable, through spectra, as phenoxyl radicals and $Ru(bpy)_3^{+}$. The spectra of transient photoproducts in two typical cases, namely, *p*-methoxyphenolate ion and *p*-methoxy-*N*,*N*-dimethylaniline as quenchers, are presented in Figure 2. The spectra can be shown to be the spectrum of $Ru(bpy)_3^{+}$ ($\lambda_{max}$ ~ 460 nm in acetonitrile)[7] in combination with that of *p*-methoxyphenoxyl radical ($\lambda_{max}$ = 415 nm in aqueous acetonitrile)[11c] for Figure 2A,B and of radical cation of *p*-methoxy-*N*,*N*-dimethylaniline ($\lambda_{max}$ = 495 nm in acetonitrile)[14] for Figure 2A′,B′.

For quenching kinetics based on laser flash photolysis, one could monitor any of the following: (i) decay of phosphorescence at 610–640 nm, (ii) decay of triplet–triplet spectral absorption at 360–380 nm, (iii) recovery of ground-state depletion at 440–460 nm, and (iv) formation of $Ru(bpy)_3^{+}$ through its absorption at 510–530 nm. Representative experimental traces as well as first-order fitting of kinetic data corresponding to each of these processes are given in Figure 3. All of the four methods give experimental first-order rate constants ($k_{obsd}$) that agree with one another within experimental errors. For the sake of consistency, we always employed the first method based on phosphorescence decay measurement as a function of quencher concentration. The quenching rate constant ($k_q$) was obtained from the plots according to the following equation:

$$k_{obsd} = k_0 + k_q[Q] \quad (1)$$

where $k_0^{-1}$ is the lifetime of $*Ru(bpy)_3^{2+}$, found, in the present

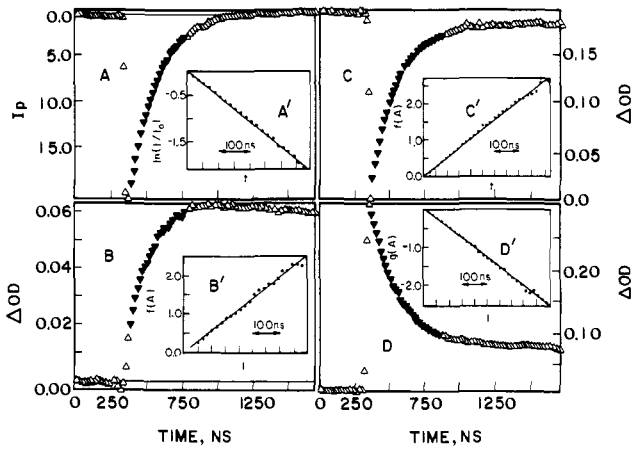


**Figure 3.** Typical experimental traces observed for Ru(bpy)$_3^{2+}$ + 0.028 M PhO$^-$ system in aqueous solution (at pH 12.7): (A) decay of phosphorescence at 630 nm, (B) formation of Ru(bpy)$_3^+$ at 510 nm, (C) recovery of ground-state depletion at 440 nm, and (D) decay of triplet–triplet absorption of Ru(bpy)$_3^{2+}$ at 368 nm. The fitting of the data into proper integrated rate equations (first order) is shown in the inset in each case. $f(A) \equiv \ln [(A_\infty - A)/A_\infty]$ for insets B′ and C′ and $g(A) \equiv \ln [(A - A_\infty)/(A_0 - A_\infty)]$ for inset D′, where $A_0$, $A_\infty$, and $A$ are Δ(OD)'s at times zero, infinity, and $t$, respectively.

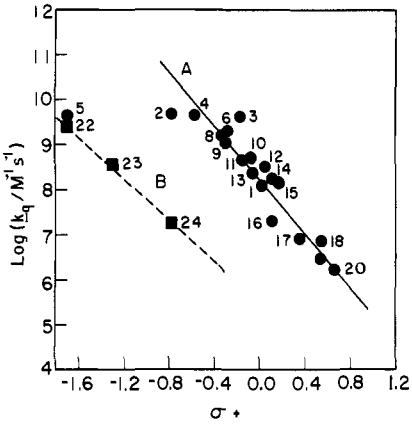


**Figure 4.** Hammett plot (A) for phenolate ions at pH 13.7 and (B) for phenols at pH 7. For the numbers identifying phenols, see Table I.

study, to be close to 600 ns in aqueous solutions. The plots of $k_{obsd}$ vs. [Q] were all reasonably linear; in particular, no supralinear behavior suggestive of ground-state association between Ru(bpy)$_3^{2+}$ and phenolate ions was observed.

The kinetic data concerning quenching by various phenolate ions are given in Table I. The rate constant for quenchingh by *p*-CN- and *p*-$COCH_3$-substituted phenolate ions was too small to be determined beyond experimental errors by the flash-photolytic observation of phosphorescence decay. In these two cases, estimates for $k_q$ were made by steady-state phosphorescence quenching with $\lambda_{ex}$ = 500 nm and $\lambda_{mon}$ = 600 nm in solutions containing the quenchers at 0.05 M.

The Hammett plots based on the $k_q$ data of phenolate ions and phenols are shown in Figure 4. The slopes of the plots give $\rho^+ = -3.0$ for phenolate ions and −2.3 for phenols.

**Electron Transfer Yields.** The electron transfer yield ($\eta$) is defined as the fraction of quenching events that result in photoreduction and is determined by using relationships 2a and 2b. In

$$\eta = \frac{[Ru(bpy)_3^+]_\infty}{[^*Ru(bpy)_3^{2+}]_0} \frac{k_{obsd}}{k_{obsd} - k_0} \quad (2a)$$

$$= \frac{\Delta(OD)_\infty^{\lambda_1}}{\Delta(OD)_0^{\lambda_2}} \frac{\Delta\epsilon^*_{\lambda_2}}{\Delta\epsilon^P_{\lambda_1}} \frac{k_{obsd}}{k_{obsd} - k_0} \quad (2b)$$

these relationships, $\Delta(OD)_\infty^{\lambda_1}$ is the net absorbance change observed following the completion of *Ru(bpy)$_3^{2+}$ decay at the wavelength $\lambda_1$ where the spectral absorption due to photoproduct(s) is relatively intense, $\Delta\epsilon^P_{\lambda_1}$ is the change in extinction coefficients at $\lambda_1$ on going from ground-state Ru(bpy)$_3^{2+}$ to the photoproduct(s), $\Delta(OD)_0^{\lambda_2}$ is the end-of-pulse absorbance change at wavelength $\lambda_2$ where *Ru(bpy)$_3^{2+}$ absorption dominates, and $\Delta\epsilon^*_{\lambda_2}$ is the difference of extinction coefficients of *Ru(bpy)$_3^{2+}$ and Ru(bpy)$_3^{2+}$ at $\lambda_2$. For all of our measurements we have used 510 nm for $\lambda_1$, 368 nm for $\lambda_2$, and 20 000 M$^{-1}$ cm$^{-1}$ for $\Delta\epsilon^*_{368}$. When Ru(bpy)$_3^+$ was the sole photoproduct that absorbed at 510 nm, $\Delta\epsilon^P_{510}$ was taken to be 10 400 M$^{-1}$ cm$^{-1}$. With some quenchers, viz., *p*-methoxy-*N*,*N*-dimethylaniline and phenols with such substituents as $N(CH_3)_2$, $NH_2$, $C_6H_5$, and I in the para positions, the contribution of the spectral absorption from the quencher-derived radical or radical ion was nonnegligible at 510 nm. In such cases, the extinction coefficients due to the radical or radical cation at 510 nm were estimated by photoreducing benzophenone with these quenchers in 1:1 water/acetonitrile (containing ~0.001 M NaOH except when *p*-methoxy-*N*,*N*-dimethylaniline was used) and comparing the absorbance changes at 510 nm with those at 640–660 nm (due to benzophenone radical anion, $\epsilon_{max}$ = 7500 M$^{-1}$ cm$^{-1}$). In particular, the extinction coefficient of the radical cation of *p*-methoxy-*N*,*N*-dimethylaniline at 510 nm was found to be quite high, viz., (8 ± 1) × 10$^3$ M$^{-1}$ cm$^{-1}$.

Table I. Kinetic and Yield Data Concerning *Ru(bpy)$_3^{2+}$ Quenching by Phenolic Compounds and Reaction of Ru(bpy)$_3^+$ with Phenoxyl Radicals at 23 °C in Aqueous Solution ($\mu$ = 0.05)

| quencher | $10^{-9}k_q$,[a,d] M$^{-1}$ s$^{-1}$ | $\eta$[b,d] | $10^{-9}k_b$,[c,d] M$^{-1}$ s$^{-1}$ |
|---|---|---|---|
| substituent(s) in phenolate ion[e] | | | |
| none (1) | 0.12 | 0.53 | 5.3 |
| *p*-$OCH_3$ (2) | 4.5 | 0.40 | 12 |
| *p*-$C_6H_5$ (3) | 4.5 | 0.46 | 7.6 |
| *p*-$OCH_2CH_3$ (4) | 4.4 | 0.44 | 12 |
| *p*-$N(CH_3)_2$ (5) | 3.9 | 0.42 | |
| *p*-$CH_2CH_3$ (6) | 1.8 | 0.56 | 7.2 |
| 2,4,6-trimethyl (7) | 1.6 | 0.36 | 12 |
| *p*-$CH_3$ (8) | 1.5 | 0.60 | 11 |
| *p*-$C(CH_3)_3$ (9) | 1.2 | 0.67 | 12 |
| *m*-$CH_3$ (10) | 0.47 | 0.61 | 8.1 |
| *p*-I (11) | 0.42 | 0.14 | 11 |
| *m*-$OCH_3$ (12) | 0.33 | 0.44 | 7.2 |
| *p*-F (13) | 0.21 | 0.60 | |
| *p*-Cl (14) | 0.19 | 0.65 | 10 |
| *p*-Br (15) | 0.17 | 0.35 | 10 |
| *p*-$COO^-$ (16) | 0.021 | 0.57 | 9.8 |
| *m*-F (17) | 0.0085 | 0.95 | |
| *m*-CN (18) | 0.0082 | | |
| *p*-$COCH_3$ (19) | ~0.003[g] | | |
| *p*-CN (20) | ≤0.002[g] | | |
| other quenchers[f] | | | |
| *p*-methoxy-*N*,*N*-dimethylaniline (21) | 2.6 | 0.58 | 9.6 |
| *p*-hydroxy-*N*,*N*-dimethylaniline (22) | 2.4 | 0.52 | |
| *p*-hydroxyaniline (23) | 0.38 | 0.68 | |
| *p*-methoxyphenol (24) | 0.018 | 0.80 | |

[a] *Ru(bpy)$_3^{2+}$ quenching rate constant. [b] Yield of Ru(bpy)$_3^+$. [c] Rate constant for Ru(bpy)$_3^+$ + ArO·. [d] Estimated variations, based on three measurements in typical cases, are ±15%, ±20%, and ±25% for $k_q$, $\eta$, and $k_b$, respectively. [e] At pH 12.7. [f] At pH 7. [g] Estimated from luminescence quenching.

Table I contains the electron transfer yield data obtained at a single concentration, [Q], of each quencher such that $k_{obsd}$ was 2–4 times larger than $k_0$. No definitive correlation is noted between $\eta$ and $k_q$ (or substituent in the phenol). Among the halogen-substituted phenols, $\eta$ decreases in the order *p*-Cl ~ *p*-F < *p*-Br < *p*-I, suggesting a heavy-atom effect. A similar effect has also been observed[11a,c] in the photoreduction of benzophenone by phenols and phenolate ions.

**Back Electron Transfer Reactions among the Photoproducts.** In most cases, the absorption due to Ru(bpy)$_3^+$ at 510–530 nm was found to decay on a relatively long time scale (100–200 μs)

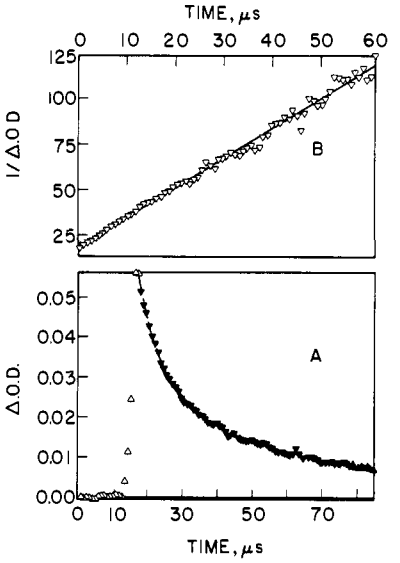


**Figure 5.** (A) Experimental trace for decay of $Ru(bpy)_3^{+}$ formed by photoreduction by phenolate ion in aqueous solution at pH 12.7 and monitored at 510 nm. (B) Fitting of the data in (A) into the integrated equation based on second-order, equal-concentration kinetics.

with kinetics that could be fitted reasonably well into the integrated rate equation for a second-order, equal-concentration reaction. This was true for a majority of the phenolate ions at pH 12–13. The dominant mode of decay of $Ru(bpy)_3^{+}$ appears to be the back electron transfer to the quencher-derived radical or radical ion, shown in eq 3.

$$Ru(bpy)_3^{+} + ArO\cdot \xrightarrow{k_b} Ru(bpy)_3^{2+} + ArO^{-} \qquad (3)$$

Figure 5A shows the experimental trace for the decay of $Ru(bpy)_3^{+}$ following its formation through reductive quenching by phenolate ion. Figure 5B shows the plot based on $\Delta(OD)^{-1} = \Delta(OD)_0^{-1} + k_b(\Delta\epsilon^{P}_{\lambda_1} l)^{-1} t$, where $l$ is the path length of the photolysis cell (0.3 cm), and $\Delta(OD)$ and $\Delta(OD)_0$ are absorbance changes at time $t$ and zero, respectively.

$k_b$ data, obtained with several phenoxyl radicals as reacting species for $Ru(bpy)_3^{+}$ at high pH, are summarized in Table I. Evidently the magnitudes of $k_b$ are in the range $5 \times 10^9$–$12 \times 10^9$ $M^{-1}$ $s^{-1}$ and show no well-defined dependence on the nature of the substituent in phenoxy radicals. We should note that an important source of error in the measurement of $k_b$ lies in a small first-order component of $Ru(bpy)_3^{+}$ decay arising from quenching by trace impurities in the phenols that would remain undetected in the approximate second-order, equal-concentration kinetic fit but would contribute significantly to the calculated value for $k_b$.

**Effect of Ionic Strength.** The effect of ionic strength on electron transfer kinetics and yields has been studied by using *p*-methoxyphenolate ion and *p*-methoxy-*N*,*N*-dimethylaniline as quenchers in aqueous medium. The ionic strength of the solutions was varied by adding $NaNO_3$. As expected for a reaction between oppositely charged ions, the rate constant for $*Ru(bpy)_3^{2+}$ quenching by *p*-methoxyphenolate ion decreases as the ionic strength is increased. Figure 6A shows a plot of log $k_q$ against $\mu^{1/2}(1 + \mu^{1/2})^{-1}$ for *p*-methoxyphenolate ion. The slope of the linear portion of the plot at low ionic strengths is obtained as −1.3, compared to the theoretical value[20] of −2 for a diffusion-controlled reaction between two small ions of charge 2+ and 1−, respectively, in water at 25 °C at low ionic strengths. The quenching by *p*-methoxy-*N*,*N*-dimethylaniline also shows a small dependence on $\mu$ (Figure 6B), the effect being a slight increase in $k_q$ on increasing $\mu$. There was practically no effect of ionic strength on $*Ru(bpy)_3^{2+}$ lifetime ($k_0^{-1}$).

In the case of both *p*-methoxyphenolate ion and *p*-methoxy-*N*,*N*-dimethylaniline as quenchers, the effect of $\mu$ on electron transfer yield ($\eta$) is quite dramatic. As the data in Table II show, $\eta$ decreases systematically on increasing $\mu$; the value of $\eta$ at 5 M $NaNO_3$ solution is less than one-third of the value in the absence of the salt.

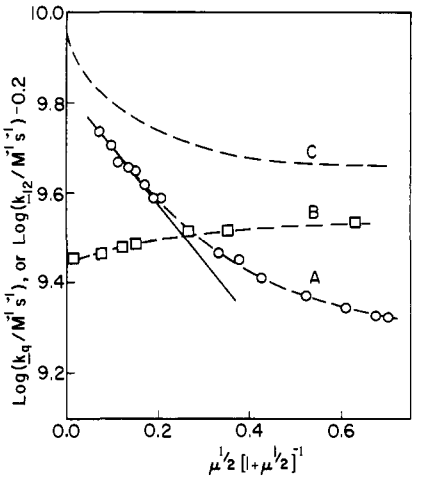


**Figure 6.** Ionic strength dependence of (A) $k_q$ for *p*-methoxyphenolate ion in aqueous solution containing 0.005 M NaOH, (B) $k_q$ for *p*-methoxy-*N*,*N*-dimethylaniline in aqueous solution, (C) rate constant for diffusional process in water between an anion of charge 1− and radius 3.8 Å and a cation of charge 2+ and radius 7.1 Å, calculated by using Debye–Smoluchowski equation.[25] For A and B, $NaNO_3$ was used as the electrolyte.

Table II. Effect of Ionic Strength on Electron Transfer Yield ($\eta$) in the Photoreduction of $Ru(bpy)_3^{2+}$ by *p*-Methoxyphenolate Ion and *p*-Methoxy-*N*,*N*-dimethylaniline in Water at 23 °C

| *p*-methoxyphenolate ion[a] | | *p*-methoxy-*N*,*N*-dimethylaniline | |
|---|---|---|---|
| $\mu$ | $\eta$[b] | $\mu$ | $\eta$[b] |
| 0.005 | 0.49 | 0.000 | 0.73 |
| 0.018 | 0.43 | 0.006 | 0.69 |
| 0.04 | 0.42 | 0.018 | 0.67 |
| 0.36 | 0.39 | 0.030 | 0.64 |
| 0.54 | 0.36 | 0.30 | 0.44 |
| 1.18 | 0.33 | 2.95 | 0.35 |
| 2.36 | 0.23 | 5.35 | 0.20 |
| 5.31 | 0.13 | | |

[a] In the presence of 0.005 M NaOH. [b] Estimated variation, ±20%.

Table III. Activation Parameters for $*Ru(bpy)_3^{2+}$ Quenching by Phenolate Ions and Reaction between $Ru(bpy)_3^{+}$ and Phenoxy Radical in Water in the Presence of 0.05 M NaOH

| reaction | $E_a$,[a] kcal/mol | log $[A/(M^{-1}\ s^{-1})]$ |
|---|---|---|
| $*Ru(bpy)_3^{2+} + p\text{-}CH_3O\text{-}C_6H_4O^{-}$ | 4.2 | 12.7 |
| $*Ru(bpy)_3^{2+} + C_6H_5O^{-}$ | 8.1 | 15.1 |
| $*Ru(bpy)_3^{2+} + p\text{-}COO^{-}\text{-}C_6H_4O^{-}$ | 12.8 | 16.9 |
| $Ru(bpy)_3^{+} + C_6H_5O\cdot$ | 3.7 | 12.5 |

[a] Based on one set of measurements with varying $ArO^{-}$ concentrations at 0–80 °C.

**Effect of Temperature.** Based on data in the temperature range 0–80 °C in aqueous solutions, activation parameters were determined for quenching by some of the phenolate ions. The Arrhenius plots, shown in Figure 7, are essentially linear in this temperature range. The data concerning activation energy ($E_a$) and preexponential factor ($A$) are presented in Table III.

The electron transfer yield ($\eta$) shows an increasing trend on raising temperature and approaches the quantitative value of unity at higher temperatures (see Table IV).

**Solvent Effect.** Using aqueous ethanol and aqueous acetone of varying compositions, we have examined the solvent effect on $k_0$, $k_q$, and $\eta$ with *p*-methoxyphenolate ion and *p*-methoxy-*N*,*N*-dimethylaniline as quenchers. The related data are presented in Table V. Interestingly, the increase in the excited-state lifetime

Scheme I

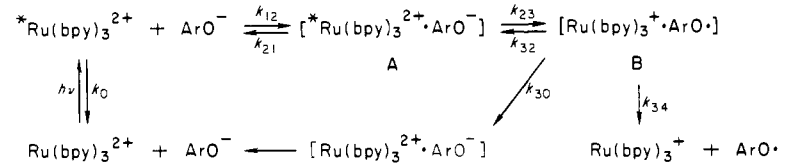


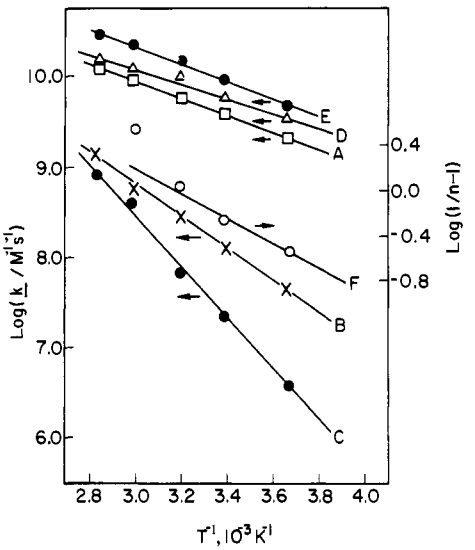


**Figure 7.** Arrhenius plots for (A) quenching by *p*-$CH_3O$-$C_6H_4O^-$, (B) quenching by $C_6H_5O^-$, (C) quenching by *p*-$COO^-$-$C_6H_4O^-$, (D) back-reaction, $Ru(bpy)_3^{+}$ + $C_6H_5O\cdot$, (E) rate constant ($k_{12}$) for diffusion in water at $\mu$ = 0.05 M between an anion of charge 1- and radius 3.8 Å and a cation of charge 2+ and radius 7.1 Å, calculated at each temperature by using Debye–Smoluchowski equation,[25] and (F) $(\eta^{-1} - 1)^{-1}$ for *p*-methoxyphenolate ion as quencher, $\eta$ being the electron transfer yield.

Table IV. Effect of Temperature on Electron Transfer Yield ($\eta$) in $Ru(bpy)_3^{2+}$ Photoreduction by Phenolate Ions in Water in the Presence of 0.05 M NaOH

| | $\eta^a$ | | |
|---|---|---|---|
| temp, °C | *p*-$CH_3O$-$C_6H_4O^-$ | $C_6H_5O^-$ | *p*-$COO^-$-$C_6H_4O^-$ |
| 0 | 0.26 | 0.38 | 0.52 |
| 23 | 0.40 | 0.53 | 0.57 |
| 40 | 0.50 | 0.75 | 0.73 |
| 60 | 0.78 | 1.0 | 0.83 |
| 80 | 1.0 | 1.1 | 1.2 |

[a] Estimated variation, ±20%. $\eta$ has been calculated by using eq 2 where $\Delta\epsilon$'s have been assumed to be constant in the temperature range 0–80 °C, and same as those at 23 °C. That this assumption is only approximately valid is shown by $\eta$ exceeding unity at higher temperatures.

($k_0^{-1}$) of $Ru(bpy)_3^{2+}$ on going from water to ethanol or acetone (95%) does not take place monotonously but goes through a maximum at intermediate solvent compositions. An analogous effect is observed for $k_q$, particularly in the case of *p*-methoxyphenolate ion as quencher in aqueous ethanol; that is, $k_q$ passes through a min. at intermediate solvent compositions. On the other hand, within the limitation of experimental errors, $\eta$ exhibits a monotonous increase on increasing the proportion of nonaqueous component (i.e., ethanol or acetone) in the solvent mixture and approaches values close to unity in solvent systems rich in the nonaqueous component. These results are illustrated in Figure 8 using the data for *p*-methoxyphenolate ion as a quencher in aqueous ethanol.

## Discussion

We propose to frame our discussion in the light of Weller's model[21] for charge transfer interaction in the excited states of molecules in a condensed phase. This model, well recognized in the current literature of excited-state electron transfer reactions, is based on a kinetic scheme where electron transfer occurs in the diffusionally produced association complex resulting in the formation of a caged pair of radicals or radical ions which, in turn, either escape from the solvent cage or undergo back electron transfer leading to the regeneration of original reactants. With $*Ru(bpy)_3^{2+}$ and $ArO^-$ as the acceptor–donor pair, the reaction scheme is shown in Scheme I.

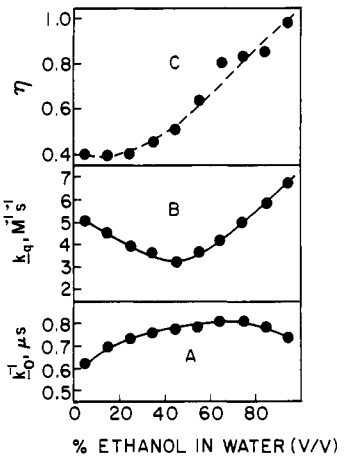


**Figure 8.** Solvent effect on (A) $Ru(bpy)_3^{2+}$ excited-state lifetime, (B) $k_q$ for *p*-methoxyphenolate ion (in the presence of 0.002 M NaOH), and (C) $\eta$ for *p*-methoxyphenolate ion (in the presence of 0.002 M NaOH), in aqueous ethanol.

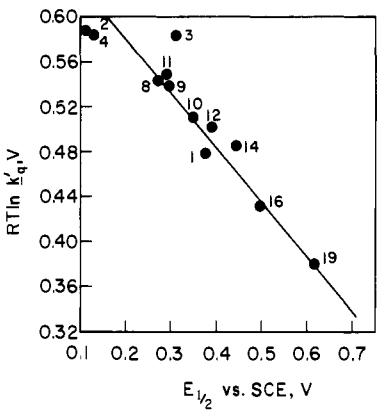


**Figure 9.** Plot based on eq 8 and 9. For the numbers identifying phenolate ions, see Table I.

Details concerning this scheme, as applied specifically to $Ru(bpy)_3^{2+}$, are given in ref 3h. The two experimental parameters, $k_q$ and $\eta$, are expressed[22] as follows:

$$k_q = k_{12}\left[1 + \frac{k_{21}}{k_{23}}\left(1 + \frac{k_{32}}{k_{34} + k_{30}}\right)\right]^{-1} \quad (4)$$

$$\eta = k_{34}/(k_{30} + k_{34}) \quad (5)$$

**Quenching Rate Constants and Free Energy Change of Electron Transfer.** In view of the fact that the triplet energy of $Ru(bpy)_3^{2+}$ ($E_T$ = 48 kcal/mol) is much lower than the lowest triplet energies of the phenolic quenchers,[23,24] the role of triplet excitation transfer in the quenching processes under examination may be considered negligible. The Hammett plots in Figure 5 show a reasonable correlation of $k_q$ with electron-releasing capability of the substituents in the phenols, except that the plot for phenolate ions

Table V. Solvent Effect on the Kinetics of Quenching of $*Ru(bpy)_3^{2+}$ by *p*-Methoxyphenolate Ion and *p*-Methoxy-*N*,*N*-dimethylaniline and the Back-Reaction between the Electron-Transfer-Derived Products[a]

| ethanol or acetone concn in water, vol % | $*Ru(bpy)_3^{2+}$ lifetime, μs | *p*-methoxyphenolate ion[b] | | | *p*-methoxy-*N*,*N*-dimethylaniline | | |
|---|---|---|---|---|---|---|---|
| | | $10^{-9}k_q$, $M^{-1}$ $s^{-1}$ | $\eta$[c] | $10^{-9}k_b$, $M^{-1}$ $s^{-1}$ | $10^{-9}k_q$, $M^{-1}$ $s^{-1}$ | $\eta$[c] | $10^{-9}k_b$, $M^{-1}$ $s^{-1}$ |
| ethanol | | | | | | | |
| 5 | 0.62 | 5.0 | 0.40 | 14 | 2.9 | 0.58 | 4.2 |
| 15 | 0.70 | 4.5 | 0.39 | | | | |
| 25 | 0.74 | 3.9 | 0.40 | | 2.7 | 0.61 | |
| 35 | 0.76 | 3.6 | 0.46 | | | | |
| 45 | 0.77 | 3.2 | 0.51 | | 2.0 | 0.87 | 1.7 |
| 55 | 0.78 | 3.7 | 0.64 | 6.1 | | | |
| 65 | 0.81 | 4.2 | 0.80 | | 1.8 | 1.0 | |
| 75 | 0.81 | 5.0 | 0.82 | | | | |
| 85 | 0.79 | 5.8 | 0.85 | 6.3 | 2.5 | 1.0 | |
| 95 | 0.74 | 6.8 | 0.98 | | 3.4 | 1.1 | 1.4 |
| acetone | | | | | | | |
| 5 | 0.61 | 4.5 | 0.42 | 14 | 3.1 | 0.58 | 5.0 |
| 15 | 0.67 | 4.4 | 0.54 | | | | |
| 25 | 0.72 | 4.3 | 0.56 | | 2.9 | 0.65 | |
| 35 | 0.77 | 4.4 | 0.72 | | | | |
| 45 | 0.79 | 4.6 | 0.80 | | 2.7 | 0.82 | 3.0 |
| 55 | 0.80 | 5.5 | 0.97 | 10 | | | |
| 60 | 0.81 | 5.8 | 0.95 | | | | |
| 65 | 0.80 | 6.5 | 1.1 | | 2.9 | 0.81 | |
| 70 | 0.81 | 7.3 | 0.98 | | | | |
| 75 | 0.81 | 8.8 | 1.1 | | | | |
| 80 | 0.80 | 10.9 | 1.3 | | | | |
| 85 | 0.77 | 14.1 | 1.3 | 14 | 3.7 | 0.80 | 6.1 |
| 90 | 0.76 | 18.1 | 1.3 | | | | |
| 95 | 0.71 | 24.4 | 1.3 | | 5.1 | 0.74 | 6.1 |

[a] Estimated variations for $\eta$, $k_q$, and $k_b$ are same as for Table I. [b] In the presence of 2 mM NaOH. [c] Calculated by using $\Delta\epsilon$ values in water; that $\Delta\epsilon$'s change slightly with solvent is indicated by $\eta$ exceeding unity in solvent mixtures rich in ethanol or acetone.

(Figure 4A) bends at large negative $\sigma$ values where $k_q$'s are in the range $4 \times 10^9$–$5 \times 10^9$ $M^{-1}$ $s^{-1}$. This result, as well as that concerning large yields of redox photoproducts ($Ru(bpy)_3^+$, ArO·, etc.), strongly establishes photoreductive charge transfer as the dominant mode of interaction involved in $*Ru(bpy)_3^{2+}$ quenching.

It is of interest to examine the relationship between the free energy change ($\Delta G_{23}$) in the electron transfer step of Scheme I and the quenching rate constants after correction of the latter for the initial diffusional process ($k_{12}$).[25] The corrected quenching rate constant, $k_q'$, is defined by eq 6 and related to the rate

$$k_q' = 1/(k_q^{-1} - k_{12}^{-1}) \quad (6)$$

$$k_q' = K_{12}Fk_{23} \quad (7)$$

constants of Scheme I by eq 7, where $K_{12} = k_{12}/k_{21}$ and $F = (k_{30} + k_{34})/(k_{30} + k_{34} + k_{32})$. Using the expression, based on Marcus–Hush theory,[26] for free energy of activation ($\Delta G^*_{23}$) for electron transfer in the association complex one can obtain the following expression for $k_q$ (for details see ref 3c and 12)

$$RT \ln k_q' = RT \ln k_q'(0) - (\Delta G_{23}/2)(1 + \Delta G_{23}/2\lambda) \quad (8a)$$

$$\ln k_q'(0) = \ln (K_{12}\nu_{23}F) - \lambda/4 \quad (8b)$$

where $k_q'(0)$ is a constant for a series of structurally and electronically analogous quenchers (provided $F \approx 1$) and may be defined as the quenching rate constant for the quencher for which $\Delta G_{23} = 0$, $\lambda/4$ is the energy barrier to electron transfer arising from reorganization of inner and outer coordination spheres, and $\nu_{23}$ is the frequency factor for electron transfer. For reductive quenching of $*Ru(bpy)_3^{2+}$ by phenolate ions $\Delta G_{23}$ in eq 8 is given by

$$\Delta G_{23} = E_{ArO\cdot/ArO^-} - E_{*Ru(bpy)_3^{2+}/Ru(bpy)3^+} + W_p - W_r \quad (9)$$

where $W$'s are the Coulombic work[28] in bringing together the reactants and products to form the association complex (A) and the ion–radical pair (B), respectively. Combined together, eq 8 and 9 imply that, in the limit $|\Delta G_{23}|$ is small compared to $\lambda$, a plot of $RT \ln k_q'$ against $E_{ArO\cdot/ArO^-}$ would be linear with slope equal to −0.5.

Figure 9 shows the plot of $RT \ln k_q'$ against phenolate redox potentials ($E_{1/2}$) at pH 12.7, calculated from the $E_{1/2}$ data[29] available for phenols in 1:1 water/2-propanol at pH 5.6. The slope of the solid straight line drawn is −0.5, suggesting that eq 8 is reasonably valid as far as the quenching mechanism with most of the phenolate ions is concerned. This result is very similar to that obtained[3a,12] for the quenching of $*Ru(bpy)_3^{2+}$ in acetonitrile by pyridinium ions (oxidative) and aromatic amines (reductive). It should be noted that the slope of −0.5 in the region centered at $\Delta G_{23} = 0$ follows also from the empirical relationship introduced by Balzani and co-workers[27] for $\Delta G^*_{23}$.

The plot in Figure 9 permits us to calculate $k_q'(0)$, since $E_{*Ru(bp])_3^{2+}/Ru(bpy)_3^+}$ in water is known (0.60 V vs. SCE). Since $W_r$ = −0.02 V[28] and $W_p = 0$ for phenolate ions, $RTk_q'(0)$ is given by the point on the plot at which phenolate redox potential is 0.58

(28) In water at 23 °C and $\mu$ = 0.05 M, $W_p = 0$ and $W_r$ is shown to be −0.02 V for a phenolate ion as the reactant. $W$'s are calculated by using the relationship $W$ in volts = $0.18Z_AZ_Ba^{-1}(1 + 0.325a\mu^{1/2})^{-1}$ where $a$ = 10.9 Å, and $Z_A$ and $Z_B$ are the charges of reactant ions (2+ and 1−).

(29) $E_{1/2}$'s for phenolate ions in water at pH 12.7 were calculated from the data[30] for phenols at pH 5.6 in 1:1 water/2-propanol using the relationship[31] $E_{1/2}$ = constant + 0.059[log ([$H^+$] + $K_D$) − log $K_D$], where $K_D$ is the acid dissociation constant of phenol in water. $K_D$'s were either available[32] or calculated from a linear relationship (least squares) between log $K_D$ and $\sigma$ (Hammett). For comparison's sake, $E_{1/2}$ value calculated for *p*-methoxyphenolate ion in this manner is 0.354 V vs. NHE, which is slightly higher than the redox potential (0.320 ± 0.02 V vs. NHE) found[33] for this phenolate ion in aqueous solution at pH 13.5 in the course of a pulse-radiolytic study of electron transfer rates and equilibria. We have assumed that the difference, ~0.03 V, which may arise because of difference in solvent conditions, remains constant for all the phenolate ions.

(30) Suatoni, J. C.; Snyder, R. E.; Clark, R. O. *Anal. Chem.* **1961**, *33*, 1894–7.

(31) (a) Hedenburg, J. F.; Frieser, H. *Anal. Chem.* **1953**, *25*, 1355–8. (b) Ilan, Y. A.; Czapski, G.; Meisel, D. *Biochim. Biophys. Acta* **1976**, *430*, 209–24.

(32) Weast, R. C., Ed. "Handbook of Chemistry and Physics", 47th ed.; Chemical Rubber Publishing Co.: Cleveland, OH 1967.

V. We thus obtain a value of 0.40 V for $RT \ln k_q'(0)$ and, hence, $5.1 \times 10^6$ $M^{-1}$ $s^{-1}$ for $k_q'(0)$. This, in turn, gives a value of $7 \times 10^4$ $M^{-1}$ $s^{-1}$ for the self-exchange rate constant[34] ($k_{11}$) for phenolate ions, based on the relationship $k_q'(0) \simeq (k_{11}k_{22})^{1/2}$ and using the value[35] of $5 \times 10^8$ $M^{-1}$ $s^{-1}$ for self-exchange rate constant ($k_{22}$) for $*Ru(bpy)_3^{2+}/Ru(bpy)_3^{+}$. Even after making allowance for approximations in this estimation,[34] we note that the self-exchange rate constant for $ArO\cdot/ArO^-$ couples is much smaller than those for aromatic amines (e.g., $k_{11} = 1.0 \times 10^9$ $M^{-1}$ $s^{-1}$ for *p*-*N*,*N*,*N*′,*N*′-tetramethylphenylenediamine in acetonitrile at 25 °C and $\mu = 0.1$ M).[36]

**Environmental Effects on Quenching Rate Constants.** Our observation that the slope of the plot log $k_q$ vs. $\mu^{1/2}(1 + \mu^{1/2})^{-1}$ in Figure 6 is smaller in magnitude than that expected from the theory suggests that probably ion pairing occurs with the reactant ions giving them smaller, nonintegral charges. Such an interpretation has indeed been given to a similar result in a study[31] concerning $*Ru(bpy)_3^{2+}$ quenching by paraquat and related doubly charged bipyridinium ions where the observed slopes have been found to be in the range 2.0–2.7 (instead of the theoretical value, 4.1). In order to check the validity of the interpretation in terms of ion pairing in our case, we have calculated $k_{12}$ (rate constant for diffusion between $Ru(bpy)_3^{2+}$ and $ArO^-$)[25] as a function of $\mu$. The result is shown in Figure 6C. Evidently, the theoretical slope of −2 is realized only at very low $\mu$ values. As a matter of fact, the observed slope (−1.3) at low $\mu$ values (Figure 6A) appears to be higher in magnitude than the slope of the theoretically calculated curve (Figure 6C) in the same ionic strength region. This comparison strongly suggests that the product of ionic charges of reactants is close to −2, and the fact that we have not observed this value is related to our inability to use sufficiently low ionic strength (owing to the requirement of using NaOH to maintain high pH).

In spite of the composite nature of $k_q$ (eq 4), its dependence on temperature follows the simple Arrhenius equation as shown in the cases of three selected phenolate quenchers (Figure 7A–C). Clearly, the temperature range (0–80 °C) used is too small and the range of experimental errors too large to show any nonlinearity in the Arrhenius plots. As expected, when the rate constants approach the limit of diffusion control as in the case of the quenching of $*Ru(bpy)_3^{2+}$ by *p*-methoxyphenolate ion and the back-reaction, $Ru(bpy)_3^{+} + PhO\cdot$, the activation energy (~4 kcal/mol) is similar to what is expected for the diffusional process (dictated primarily by the temperature dependence of solvent viscosity). The actual Arrhenius plot for the latter (Figure 7E) based on $k_{12}$ data calculated individually at each temperature for the ion–ion diffusional reaction, $*Ru(bpy)_3^{2+} + ArO^-$, is found to be parallel to the plot for the quenching of $*Ru(bpy)_3^{2+}$ by *p*-methoxyphenolate ion (Figure 7A). As $k_q$ becomes much smaller from the rate constant for the diffusional process, the apparent activation energy becomes larger, e.g., in the case of $C_6H_5O^-$ and $p\text{-}COO^-\text{–}C_6H_4O^-$ as quenchers. For these phenolate ions, $k_q' \simeq k_q$, and the contribution of the electron transfer step ($k_{23}$) is relatively important. The increase in the activation energy of this step in the order $p\text{-}OCH_3\text{–}C_6H_4O^- < C_6H_5O^- < p\text{-}COO^-\text{–}C_6H_4O^-$ correlates with the decrease in the exothermicity of electron transfer, as expected from Marcus theory.[26b]

The solvent effect on $k_q$, as observed with *p*-methoxyphenolate ion and *p*-methoxy-*N*,*N*-dimethylaniline as quenchers in aqueous ethanol and aqueous acetone, also appears to be quite interesting but complex. Noting that $k_q$ for both quenchers is close to the limit of diffusion control, the increase in $k_q$ on going from water to a substantially less polar solvent (e.g., 95% acetone or 95% ethanol in water) can be explained, at least partially, in terms of increased electrostatic interaction (cation–anion or cation-induced dipole) and its contribution to $k_{12}$ in the latter solvents. In the case of water vs. acetone, the decreased viscosity of acetone is also an important factor contributing to $k_{12}$. Also, $k_{23}$ and $k_{34}$ are expected to be larger in acetone and ethanol because of smaller $\lambda$ (owing to smaller dielectric constant and less tightly bound solvent cage). However, what cannot be understood in a straightforward manner is that $k_q$ for both quenchers goes through a minimum at intermediate solvent compositions for both aqueous ethanol and aqueous acetone, rather than changing monotonously in accordance with the gradual change of bulk properties such as viscosity and dielectric constant with solvent composition.

**Environmental Effects on Electron Transfer Yields.** The effects of various environmental factors on electron transfer yields ($\eta$) may be summarized in terms of increased $\eta$ at lower ionic strengths, in less polar solvents, and at higher temperatures. Interestingly, the results concerning solvents and ionic strengths are similar for both *p*-methoxyphenolate ion, and anionic quencher, and *p*-methoxy-*N*,*N*-dimethylaniline, a neutral quencher. For comparison's sake, the positive temperature coefficient of $\eta$ has also been found[11a] for the photoreduction of benzophenone by phenols in toluene in the temperature range −90 to 23 °C, and the increase of $\eta$ with decrease in solvent polarity has also been observed[37] for the photoreductive quenching of triplet methylene blue by Fe(II) complexes.

In terms of eq 5, $\eta$ is determined by the competition between the two processes represented by $k_{30}$ and $k_{34}$, that is, back electron transfer in the caged ion–radical pair B (followed by dissociation into starting reactants) and direct dissociation of B into photoproducts. Any change in $\eta$ with change in environmental conditions should be a reflection of changes in relative magnitudes of these two processes. The observed positive temperature coefficient of $\eta$ (Table III) suggests that $k_{34}$ has a higher activation energy than $k_{30}$. From the low-temperature portion of the plot of $-\log(1/\eta - 1)$ vs. $1/T$ (Figure 7F), it is seen that the activation energy difference for $k_{34}$ and $k_{30}$ is of the order of 3 kcal/mol. Also, qualitatively, the increase of $\eta$ on decreasing the polarity of the medium may be explained by the fact that the solvent cage for the ion–radical pair (B) is relatively weak in the less polar solvent with weaker intermolecular hydrogen bonding, rendering the process $k_{34}$ facile. In addition, with *p*-methoxyphenolate ion as the quencher, the process $k_{30}$ occurring via a dipolar transition state and the subsequent ionization are expected to be favored in a more polar solvent.

**Implication for Photogalvanic Action.** Recent studies[38] have shown that the $Ru(bpy)_3^{2+}$–thiophenolate system exhibits photogalvanic effects; the electrochemically active species is the photoreductively produced $Ru(bpy)_3^{+}$ that has a relatively long lifetime (0.33 s in acetonitrile), its back-reaction with PhS· being suppressed owing to the fast dimerization of the latter. The present study shows that photoreduction by phenolate ions may be utilized to generate $Ru(bpy)_3^{+}$ in quantitative yields under certain conditions; however, with light intensity available from an ordinary light source, the steady-state $Ru(bpy)_3^{+}$ concentration would be too small for a practical application for photocurrent generation because of fast back electron transfer reaction among the photoproducts. Nevertheless, our results concerning the environmental effects on yields and kinetics can in principle be extended to $Ru(bpy)_3^{2+}\text{–}ArS^-$ systems and should be of value as guidelines for optimum conditions for photogalvanic action in these systems.

**Acknowledgment.** We are grateful to Drs. G. L. Hug and P. Neta for valuable comments and discussions during the course of the work.

(33) Steenken, S.; Neta, P. *J. Phys. Chem.* **1979**, *83*, 1134–7.
(34) As discussed in footnote 29, the actual redox potential of phenolate ions under the conditions of our experiments may be lower than those used in Figure 9 by ~0.03 V; this would render the value of $k_{11}$ even lower.
(35) Toma, H. E.; Creutz, C. *Inorg. Chem.* **1977**, *16*, 545–50.
(36) Kowert, B. A.; Marcoux, L.; Bard, A. J. *J. Am. Chem. Soc.* **1972**, *94*, 5538–50.
(37) Ohno, T.; Lichtin, N. N. *J. Am. Chem. Soc.* **1980**, *102*, 4636–43.
(38) Miyashita, T.; Matsuda, M. *J. Phys. Chem.* **1981**, *85*, 3122–5 and references therein.